Verification of Physical Parameters in a Rigid Manipulator Wrist Model

S. Hanssen[1], G.E. Hovland[2] and T. Brogårdh[3]

[1]ABB Robotics, S-721 68 Västerås, Sweden, Email: sven.hansen@se.abb.com
[2]ABB Corp. Research, N-1375 Billingstad, Norway, E-mail: geir.hovland@no.abb.com
[3]ABB Robotics, S-721 68 Västerås, Sweden, Email: torgny.brogardh@se.abb.com

Abstract

In this paper we present an identification algorithm for the rigid-body parameters of an industrial ABB robot wrist. The main contributions of our work are 1) the demonstration of rigid-body dynamic identification algorithms on large industrial robots, for which we handle complex internal couplings of the manipulator wrist, as shown in the experiments. 2) the use of the particular non-linear structure of the wrist model to solve a larger number of physical parameters than what is possible from general linear algorithms presented in the literature, given the measurement constraints on industrial robots.

Notation

Lowercase character (n, a, b, c), (q, τ), (v, β)	triads, scalar and vectorial matrices
Boldface uppercase character $(\mathbf{I})$	dyad
Uppercase character (N, A, B, C), (M)	reference frames, dyadic matrix
Boldface lowercase character $(\mathbf{r}, \mathbf{v})$, $(\mathbf{n}_i, \mathbf{a}_i, \mathbf{b}_i, \mathbf{c}_i)$	vectors, mutually perpendicular unit vectors
q_i, $\dot{q}_i$, u_i	generalised coordinates, velocities, speeds
${}^i m$	mass of rigid body i
${}^k J_{ij}$	components of moment of inertia dyads, body k
${}^j l_i$	length, direction i, body j
G	linear transformation matrix, motor to link

1 Introduction

The demands for path-tracking accuracy of modern industrial robots are extremely high. Current applications such as spray painting, waterjet cutting, laser cutting, plasma cutting and assembly typically demand maximum path errors of only a few tenths of a millimeter while the manipulators carry loads from less than a kilogram up to several hundred kilograms. To achieve the path tracking performance required by such applications, an extremely accurate model of the robot dynamics and the payloads of the manipulator are vital. In this paper we demonstrate a method for identifying and verifying the dynamic robot model of an industrial manipulator wrist including payload parameters.

The identification of rigid body robot dynamics has received a significant amount of attention in the literature, see for example [2, 5, 9, 11]. For most of these papers, only a subset of the physical parameters, such as mass centres, arm inertias, etc., can be identified. The remaining unknown parameters appear as linear or non-linear combinations in the identification algorithms, see section 2. Atkeson, An and Hollerback [2] describe one identification concept where 6-dof force/torque sensors are located at every single joint of the manipulator. For this case it is possible to identify all the physical parameters. However, the mounting of a 6-dof force sensor at every single joint is cumbersome and highly undesirable from a practical viewpoint.

The main contributions of our work are 1) the demonstration of rigid-body dynamic identification algorithms on large industrial robots, for which we also handle complex internal couplings of the manipulator wrist, as shown in the experiments. 2) the use of the particular non-linear structure of the wrist model to solve a larger number of physical parameters than what is possible from general linear algorithms presented in [2, 11]. The wrist model contains 25 physical parameters. From these, 18 physical

parameters can be identified directly. The remaining 7 parameters can be verified through linear and non-linear combinations. In our work these 7 parameters are verified against mechanical data obtained through CAD modelling at ABB Robotics. Mechanical data can also be obtained by measuring the individual parts of the wrist before assembly. However, some of the parameters will change after assembly due to the addition of oil and bearings. Hence, verification of the model after assembly of all parts is highly desirable.

2 Analytic Wrist Model

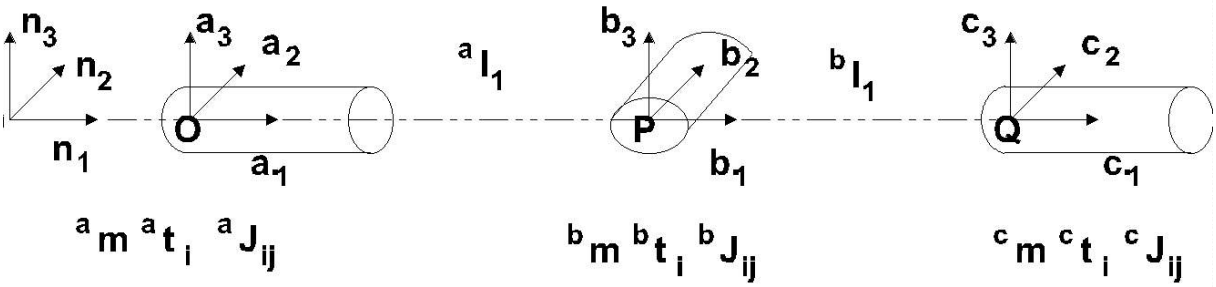

Figure 1: *Specification of wrist coordinate system and physical parameters for the 3 wrist axes, 1-3. The wrist model contains* 32 *physical parameters, of which* 25 *appear in the dynamic equations of motion.*

In this section we derive a 3-dof wrist model in which no internal couplings are considered. Then we add internal couplings, and this model we use for identification after transforming the motor variables to the arm side. The transformations of motor variables are described in section 5. The derivation of equations of motion was done in Sophia, developed by Lesser[8], with Kane's method [6]. Sophia is a set of routines to derive kinematics and dynamics in Maple. In section 2.1 we describe the kinematics of an ABB industrial robot wrist. In section 2.2 the analytical equations of motion are derived.

2.1 Kinematics

We introduce $n = \begin{pmatrix} \mathbf{n}_1 & \mathbf{n}_2 & \mathbf{n}_3 \end{pmatrix}$ as a reference triad and an origin ($\mathbf{O}$) for the inertial reference frame N. The configuration relative to the reference frame N can be written in terms of a set of independent *generalised coordinates* $q = \begin{pmatrix} q_1 & q_2 & q_3 \end{pmatrix}^T$. We introduce the reference triads, see Figure 1, as

- a rotated relative n an amount q_1 about the common $\mathbf{n}_1$-direction, a is attached to rigid body a,
- b rotated relative a an amount q_2 about the common $\mathbf{a}_2$-direction, b is attached to rigid body b,
- c rotated relative b an amount q_3 about the common $\mathbf{b}_1$-direction, c is attached to rigid body c.

The position vectors relative N of the contact points between the rigid bodies are

$$\mathbf{r}^{OP} = {}^a l_1 \mathbf{a}_1, \ \mathbf{r}^{OQ} = \mathbf{r}^{OP} + {}^b l_1 \mathbf{b}_1$$

where O, P and Q are the points shown in Figure 1. The position vectors relative N of the centre of mass for the rigid bodies are

$$\mathbf{r}^{OCMa} = a \begin{pmatrix} {}^a t_1 & {}^a t_2 & {}^a t_3 \end{pmatrix}^T, \ \mathbf{r}^{OCMb} = \mathbf{r}^{OP} + b \begin{pmatrix} {}^b t_1 & {}^b t_2 & {}^b t_3 \end{pmatrix}^T, \ \mathbf{r}^{OCMc} = \mathbf{r}^{OQ} + c \begin{pmatrix} {}^c t_1 & {}^c t_2 & {}^c t_3 \end{pmatrix}^T$$

The rigid body velocities for each body's centre of mass and the angular velocities for each body, all relative to N, are given by

$$v = \begin{pmatrix} \mathbf{v}^{CMa} \\ {}^N\boldsymbol{\omega}^A \\ \mathbf{v}^{CMb} \\ {}^N\boldsymbol{\omega}^B \\ \mathbf{v}^{CMc} \\ {}^N\boldsymbol{\omega}^C \end{pmatrix} = \begin{pmatrix} -{}^a t_3 \dot{q}_1 \mathbf{a}_2 + {}^a t_2 \dot{q}_1 \mathbf{a}_3 \\ \dot{q}_1 \mathbf{a}_1 \\ \left(-{}^b t_2 s_2 \dot{q}_1 + {}^b t_3 \dot{q}_2\right) \mathbf{b}_1 + \left({}^b t_1 s_2 \dot{q}_1 - {}^b t_3 c_2 \dot{q}_1\right) \mathbf{b}_2 + \left({}^b t_2 c_2 \dot{q}_1 - {}^b t_1 \dot{q}_2\right) \mathbf{b}_3 \\ \dot{q}_1 \mathbf{a}_1 + \dot{q}_2 \mathbf{b}_2 \\ {}^b l_1 s_2 \dot{q}_1 \mathbf{b}_2 - {}^b l_1 \dot{q}_2 \mathbf{b}_3 + \left({}^c t_2 \left(s_3 \dot{q}_2 - s_2 c_3 \dot{q}_1\right) + {}^c t_3 \left(s_2 s_3 \dot{q}_1 + c_3 \dot{q}_2\right)\right) \mathbf{c}_1 + \\ \left({}^c t_1 \left(s_2 c_3 \dot{q}_1 - s_3 \dot{q}_2\right) - {}^c t_3 \left(c_2 \dot{q}_1 + \dot{q}_3\right)\right) \mathbf{c}_2 + \left({}^c t_2 \left(c_2 \dot{q}_1 + \dot{q}_3\right) - {}^c t_1 \left(c_3 \dot{q}_2 + s_2 s_3 \dot{q}_1\right)\right) \mathbf{c}_3 \\ \dot{q}_1 \mathbf{a}_1 + \dot{q}_2 \mathbf{b}_2 + \dot{q}_3 \mathbf{c}_1 \end{pmatrix}$$

where $c_i = \cos(q_i)$ and $s_i = \sin(q_i)$. With the trivial kinematic differential equations $\dot{q}_i = u_i$ we find (by inspection) the matrix β, with tangent vectors as elements, as

$$\beta = \begin{pmatrix} -{}^a t_3 \mathbf{a}_2 + {}^a t_2 \mathbf{a}_3 & \mathbf{0} & \mathbf{0} \\ \mathbf{a}_1 & \mathbf{0} & \mathbf{0} \\ -{}^b t_2 s_2 \mathbf{b}_1 + \left({}^b t_1 s_2 - {}^b t_3 c_2 \right) \mathbf{b}_2 + {}^b t_2 c_2 \mathbf{b}_3 & {}^b t_3 \mathbf{b}_1 - {}^b t_1 \mathbf{b}_3 & \mathbf{0} \\ \mathbf{a}_1 & \mathbf{b}_2 & \mathbf{0} \\ {}^b l_1 s_2 \mathbf{b}_2 + \left(-{}^c t_2 s_2 c_3 + {}^c t_3 s_2 s_3 \right) \mathbf{c}_1 + & -{}^b l_1 \mathbf{b}_3 + \left({}^c t_2 s_3 + {}^c t_3 c_3 \right) \mathbf{c}_1 & -{}^c t_3 \mathbf{c}_2 + {}^c t_2 \mathbf{c}_3 \\ \left({}^c t_1 \left(s_2 c_3 \right) - {}^c t_3 c_2 \right) \mathbf{c}_2 + \left({}^c t_2 c_2 - {}^c t_1 s_2 s_3 \right) \mathbf{c}_3 & -{}^c t_1 s_3 \mathbf{c}_2 - {}^c t_1 c_3 \mathbf{c}_3 & \\ \mathbf{a}_1 & \mathbf{b}_2 & \mathbf{c}_1 \end{pmatrix}$$

For a detailed explanation of tangent vectors, see [7, 8].

2.2 Dynamics

To develop the dynamics, the velocity vectors (v) and tangent vectors (β) from the previous section are used. The momentum is the row matrix

$$p = v^T \bullet M = \begin{pmatrix} {}^a m \mathbf{v}^{CMa} & \mathbf{I}^{CMa} \bullet^N \boldsymbol{\omega}^A & {}^b m \mathbf{v}^{CMb} & \mathbf{I}^{CMb} \bullet^N \boldsymbol{\omega}^B & {}^c m \mathbf{v}^{CMc} & \mathbf{I}^{CMc} \bullet^N \boldsymbol{\omega}^C \end{pmatrix},$$

where M is a matrix with each rigid body along the diagonal and ${}^i m$ and $\mathbf{I}^{CMi}$ are the rigid body mass and moment of the inertia dyad, respectively. The first coloumn vector of p equals the linear momentum of body a, and the second coloumn vector of p equals the angular momentum of body a. The following elements of p describe the same momentum for body b and c. The applied forces on the system are generated by the gravitational acceleration and the motor torque in the joints

$$F_a = \begin{pmatrix} -{}^a m \mathbf{n}_3 & \tau_1 \mathbf{a}_1 & -{}^b m \mathbf{n}_3 & \tau_2 \mathbf{b}_2 & -{}^c m \mathbf{n}_3 & \tau_3 \mathbf{c}_1 \end{pmatrix}$$

By differentiation of the momentum with respect to time relative to N, we obtain the equations of motions (projected onto the tangent vector space) as

$$\left(F_a - \frac{{}^N dp}{dt} \right) \bullet \beta = \begin{pmatrix} 0 & 0 & 0 \end{pmatrix}$$

Above, we have used d'Alembert principle of virtual work on the constraint forces which gives $F_c \bullet \beta = \begin{pmatrix} 0 & 0 & 0 \end{pmatrix}$. The projected equations of motions are written as

$$J_{ij} \ddot{q}_j + S_{ijk} \dot{q}_j \dot{q}_k + g_i = \tau_i \tag{1}$$

where we used free and dummy index notation and the summation convention, see Fung [4]. The individual terms in the equation above are given as follows:

$$\begin{aligned}
g_1 &= PG_1 s_1 s_2 + PG_2 s_1 c_2 s_3 + PG_3 s_1 c_2 c_3 + PG_4 s_1 c_2 + PG_5 s_1 + PG_6 c_1 + PG_7 c_1 s_3 + PG_8 c_1 c_3 \\
g_2 &= PG_9 s_2 s_3 c_1 + PG_{10} s_2 c_1 c_3 + PG_{11} s_2 c_1 + PG_{12} c_2 c_1 \\
g_3 &= PG_{13} s_1 c_3 + PG_{14} s_1 s_3 + PG_{15} c_1 c_2 s_3 + PG_{16} c_1 c_2 c_3 \\
J_{11} &= PJ_1 s_3^2 s_2^2 + PJ_2 s_3 c_3 s_2^2 + PJ_3 s_2^2 + PJ_4 s_2 c_2 s_3 + PJ_5 c_2 s_2 c_3 + PJ_6 c_2 s_2 + PJ_7 \\
J_{12} &= PJ_8 s_2 s_3^2 + PJ_9 s_2 s_3 c_3 + PJ_{10} s_2 + PJ_{11} c_2 s_3 + PJ_{12} c_2 c_3 + PJ_{13} c_2 \\
J_{13} &= PJ_{14} s_2 s_3 + PJ_{15} s_2 c_3 + PJ_{16} c_2 \\
J_{22} &= PJ_{17} c_3 s_3 + PJ_{18} c_3^2 + PJ_{19}, \;\; J_{23} = PJ_{20} s_3 + PJ_{21} c_3, \;\; J_{33} = PJ_{22}, \;\; J_{31} = J_{13}, \;\; J_{32} = J_{23} \\
S_{111} &= S_{121} = S_{131} = S_{132} = S_{212} = S_{221} = S_{222} = S_{223} = S_{231} = S_{232} = S_{313} = S_{321} = S_{323} = \\
&\quad S_{331} = S_{332} = S_{333} = 0 \\
S_{112} &= PS_1 s_3 c_3 s_2 c_2 + PS_2 c_3^2 s_2 c_2 + PS_3 s_2 c_2 + PS_4 c_2^2 s_3 + PS_5 c_2^2 c_3 + PS_6 c_2^2 + PS_7 s_3 + \\
&\quad PS_8 c_3 + PS_9 \\
S_{113} &= PS_{10} s_3 s_2 c_2 + PS_{11} c_3 s_2 c_2 + PS_{12} s_3 c_3 c_2^2 + PS_{13} c_2^2 c_3^2 + PS_{14} c_2^2 + PS_{15} s_3 c_3 + \\
&\quad PS_{16} c_3^2 + PS_{17} \\
S_{122} &= PS_{18} s_3 s_2 + PS_{19} c_3 s_2 + PS_{20} s_2 + PS_{21} s_3 c_3 + PS_{22} c_3^2 + PS_{23} c_2 \\
S_{123} &= PS_{24} s_3 c_3 s_2 + PS_{25} c_3^2 s_2 + PS_{26} s_2, \;\; S_{133} = PS_{27} s_2 s_3 + PS_{28} s_2 c_3
\end{aligned}$$

$$
\begin{aligned}
S_{211} &= PS_{29}s_3c_3s_2c_2 + PS_{30}c_3^2s_2c_2 + PS_{31}s_2c_2 + PS_{32}c_2^2s_3 + PS_{33}c_2^2c_3 + PS_{34}c_2^2 + \\
&\quad PS_{35}s_3 + PS_{36}c_3 + PS_{37} \\
S_{213} &= PS_{38}s_3c_3s_2 + PS_{39}c_3^2s_2 + PS_{40}s_2, \;\; S_{233} = PS_{41}s_3 + PS_{42}c_3 \\
S_{311} &= PS_{43}s_3s_2c_2 + PS_{44}c_3s_2c_2 + PS_{45}c_3s_3 + PS_{46}c_3^2c_2^2 + PS_{47}c_2^2 + PS_{48}s_3c_3 + PS_{49}c_3^2 + PS_{50} \\
S_{312} &= PS_{51}s_3c_3s_2 + PS_{52}c_3^2s_2 + PS_{53}s_2 + PS_{54}c_2s_3 + PS_{55}c_2c_3 \\
S_{322} &= PS_{56}s_3c_3 + PS_{57}c_3^2 + PS_{58}
\end{aligned}
$$

The 96 parameters (PG, PJ and PS) above are defined by a set of physical parameters introduced in the model (see kinematics and dynamics above). The following 18 independent equations were found:

$$
\begin{aligned}
PG_1 &= ({}^cm{}^bl_1 + {}^c m{}^ct_1 + {}^b m{}^bt_1) \\
PG_2 &= -{}^cm{}^ct_2, \;\; PG_3 = -{}^cm{}^ct_3, \;\; PG_4 = -{}^bm{}^bt_3, \;\; PG_5 = -{}^am{}^at_3 \\
PG_6 &= {}^am{}^at_2 + {}^b m{}^bt_2 \\
PJ_1 &= {}^cJ_{22} - {}^c J_{33} + {}^c m(-{}^ct_2^2 + {}^c t_3^2), \;\; PJ_2 = 2({}^cJ_{23} - {}^c m{}^ct_2^ct_3) \\
PJ_3 &= {}^bJ_{33} - {}^c J_{11} - {}^b J_{11} + {}^c J_{33} + {}^b m({}^bt_1^2 - {}^b t_3^2) + {}^c m(2{}^bl_1^ct_1 + {}^b l_1^2 + {}^c t_1^2 - {}^c t_3^2) \\
PJ_4 &= 2({}^cJ_{12} - {}^c m{}^ct_2({}^bl_1 + {}^c t_1)), \;\; PJ_5 = 2({}^cJ_{13} - {}^c m{}^ct_2({}^bl_1 + {}^c t_1)), \;\; PJ_6 = 2({}^bJ_{13} - {}^b m{}^bt_1^bt_3) \\
PJ_7 &= {}^aJ_{11} + {}^b J_{11} + {}^c J_{11} + {}^a m({}^at_2^2 + {}^a t_3^2) + {}^b m({}^bt_2^2 + {}^b t_3^2) + {}^c m({}^ct_2^2 + {}^c t_3^2) \\
PJ_{10} &= {}^bJ_{23} - {}^c m{}^ct_2^ct_3 - {}^b m{}^bt_2^bt_3 + {}^c J_{23}, \;\; PJ_{13} = {}^b J_{12} - {}^b m{}^bt_1^bt_2, \;\; PJ_{16} = {}^c J_{11} + {}^c m({}^ct_2^2 + {}^c t_3^2) \\
PJ_{19} &= {}^bJ_{22} + {}^c J_{33} + {}^b m({}^bt_1^2 + {}^b t_3^2) + {}^c m({}^bl_1^2 + {}^c t_1^2 + {}^c t_2^2 + 2{}^bl_1^ct_1) \\
PS_3 &= 2\left(-{}^bJ_{11} + {}^b J_{33} - {}^c J_{11} + {}^c J_{22} + {}^b m({}^bt_1^2 - {}^b t_3^2) + {}^c m({}^bl_1^2 + 2{}^ct_1^bl_1 + {}^c t_1^2 - {}^c t_2^2)\right)
\end{aligned}
$$

3 Verification of Physical Parameters

Several authors have developed methods for identifying mechanical parameters, see for example [2, 5, 9, 11]. These papers, however, identify parameters of the type defined by the equations above, eg. PG_1 to PS_3, or the methods require force/torque sensors to be located at the robot's joints. In the following sections we describe the identification procedure in a practical setting at an industrial robot manufacturer. For most industrial robots, no external force/torque measurements are available. For the results presented here, only the motor torques and positions are measured. The joint velocities and acceleration data are obtained afterwards by filtering. Special care is taken to avoid phase shifts in velocity and acceleration, by using both forwards and backwards filtering of the position data.

As seen in section 2, the wrist model contains only 18 independent parameter equations, while 25 physical model parameters appear in the same equations. Hence, all these 25 physical parameters can not be solved simultaneously. However, the 18 independent equations can be used to verify linear and nonlinear combinations of the wrist's physical parameters obtained from CAD data. For example, if the identified parameter PG_2 and the corresponding estimated value from CAD data show large differences, the mechanical engineers get important feedback that either the value of ${}^cm$ or ${}^ct_2$ (or both) is wrong. The CAD data can then be modified or individual parts in a disassembled wrist can be measured more precisely using external measuring devices in an attempt to make the correspondance better. Having accurate CAD data is important for many reasons, including robot simulation studies and optimisation of motors and mechanical arm structures.

Note that the original wrist model illustrated in Figure 1 contains as many as 32 physical parameters. When modelling the wrist, 7 of these parameters (${}^at_1$,${}^a l_1$,${}^a J_{22}$,${}^a J_{33}$,${}^a J_{12}$,${}^a J_{13}$ and ${}^aJ_{23}$) disappear from the dynamic equations of motion. Hence, these 7 parameters are impossible to identify with the three motors configured as illustrated in Figure 1. When considering the complete 6-dof robot dynamic model, these 7 parameters appear in the equations and can potentially be identified. The problem of "invisible" parameters does, however, not disappear when considering the complete dynamics. As for the 3-dof dynamics, physical parameters belonging to the first axis of the robot will also disappear for the 6-dof dynamics.

The robot's control system uses the dynamic equations of motion to improve the wrist's path tracking accuracy. The 7 physical parameters which disappear from the equations will have no effect on the motion characteristics when only wrist motions is considered.

4 Identification of Model Parameters

In the previous sections we showed that it is possible to verify identified parameters against mechanical CAD data to discover errors in the modelled equations of motion. In this section, we identify 18 physical parameters by assuming that 7 of the physical wrist parameters are known in advance, for example by measurement before the wrist is assembled. The selection of these 7 parameters is not random. The physical parameters can be divided into three groups: 1) Masses and link lenghs, which are easy to measure, 2) mass centres and 3) inertia terms. When choosing the physical parameters which need to be measured before assembly, as many as possible should be from category 1) and 2) and as few as possible from category 3). In order to identify inertia terms before assembling the wrist, dedicated rotating machinery is required.

Given ${}^{a}m$,${}^{b}m$, ${}^{b}l_1$, ${}^{b}t_2$, ${}^{c}t_1$, the following solutions were found:

$$
\begin{aligned}
{}^{c}m &= \frac{-PG_2^2 + PG_3^2}{PJ_3 - \frac{1}{2}PS_3 + PJ_1} \\
{}^{c}t_2 &= -\frac{PG_2}{{}^{c}m},\ {}^{c}t_3 = -\frac{PG_3}{{}^{c}m},\ {}^{b}t_3 = -\frac{PG_4}{{}^{b}m},\ {}^{a}t_3 = -\frac{PG_5}{{}^{a}m} \\
{}^{a}t_2 &= \frac{1}{{}^{a}m}(PG_6 - {}^{b}m\,{}^{b}t_2),\ {}^{b}t_1 = \frac{1}{{}^{b}m}(PG_1 - {}^{c}m\,{}^{b}l_1 - {}^{c}m\,{}^{c}t_1) \\
{}^{c}J_{11} &= PJ_{16} - {}^{c}m({}^{c}t_2^2 + {}^{c}t_3^2),\ {}^{c}J_{23} = \frac{1}{2}PJ_2 + {}^{c}m\,{}^{c}t_2\,{}^{c}t_3 \\
{}^{b}J_{23} &= PJ_{10} + {}^{c}m\,{}^{c}t_2\,{}^{c}t_3 + {}^{b}m\,{}^{b}t_2\,{}^{b}t_3 - {}^{c}J_{23},\ {}^{b}J_{13} = \frac{1}{2}PJ_6 + {}^{b}m\,{}^{b}t_1\,{}^{b}t_3 \\
{}^{c}J_{12} &= \frac{1}{2}PJ_4 + {}^{c}m\,{}^{b}l_1\,{}^{c}t_2 + {}^{c}m\,{}^{c}t_1\,{}^{c}t_2,\ {}^{c}\mathrm{J}_{13} = \frac{1}{2}\mathrm{PJ}_5 + {}^{c}\mathrm{m}\,{}^{c}\mathrm{t}_1\,{}^{c}\mathrm{t}_3 + {}^{c}\mathrm{m}\,{}^{b}\mathrm{l}_1\,{}^{c}\mathrm{t}_3 \\
{}^{b}J_{12} &= PJ_{13} + {}^{b}m\,{}^{b}t_1\,{}^{b}t_2
\end{aligned}
$$

Given ${}^{b}J_{33}$ and ${}^{c}J_{33}$ we find the remaining 4 parameters:

$$
\begin{aligned}
{}^{c}J_{22} &= PJ_1 + {}^{c}J_{33} - {}^{c}m(-{}^{c}t_2^2 + {}^{c}t_3^2) \\
{}^{b}J_{22} &= PJ_{19} - {}^{c}J_{33} - {}^{b}m({}^{b}t_1^2 + {}^{b}t_3^2) - {}^{c}m({}^{b}l_1^2 + {}^{c}t_1^2 + {}^{c}t_2^2 + 2{}^{b}l_1^{c}t_1) \\
{}^{b}J_{11} &= -PJ_3 + {}^{b}J_{33} - {}^{c}J_{11} + {}^{c}J_{33} + {}^{b}m({}^{b}t_1^2 - {}^{b}t_3^2) + {}^{c}m(2{}^{b}l_1^{c}t_1 + {}^{b}l_1^2 + {}^{c}t_1^2 - {}^{c}t_3^2) \\
{}^{a}J_{11} &= -PJ_7 + {}^{b}J_{11} + {}^{c}J_{11} + {}^{a}m({}^{a}t_2^2 + {}^{a}t_3^2) + {}^{b}m({}^{b}t_2^2 + {}^{b}t_3^2) + {}^{c}m({}^{c}t_2^2 + {}^{c}t_3^2)
\end{aligned}
$$

The general solution given above, requires 2 masses, 1 link length, 2 mass centres and 2 inertia terms to be measured before assembling the wrist. The remaining 18 physical parameters can then be identified by excitation of the wrist motors on the final assembled wrist.

5 Experiments

Figure 2 shows measurements taken from the wrist motors which are transformed to link angles. To transform from motor variables to link side variables the following linear transformations are used

$$
\tau_a = G^T\tau_m, \quad \mathrm{q_m = Gq_a} \qquad\qquad G = \begin{pmatrix} G_{11} & 0 & 0 \\ G_{21} & G_{22} & 0 \\ G_{31} & G_{32} & G_{33} \end{pmatrix}
$$

where τ_m is a 3×1 motor torque vector, τ_a is a 3×1 torque vector transformed to the link side and q_m and q_a are the corresponding motor and link angles, respectively. The matrix G is the transmission matrix. For a detailed description of the physical design of such wrist transmissions, see Craig [3], Figure 8.8, page 271. In addition to the rigid-body parameters which we have modelled as a function of the link variables in this paper, the friction appears and needs to be modelled and identified as well. Friction identification, however, is outside the scope of this paper. A good reference on friction modelling is Armstrong-Hélouvry[1]. If we include a simple friction model on the motor side consisting of Coloumb friction only, the motion dynamics on the arm side in (1) must be modified as follows.

$$
J_{ij}\ddot{q}_j + S_{ijk}\dot{q}_j\dot{q}_k + g_i + G_{ji}C_{jk}sgn(\dot{q}_k) = \tau_i
$$

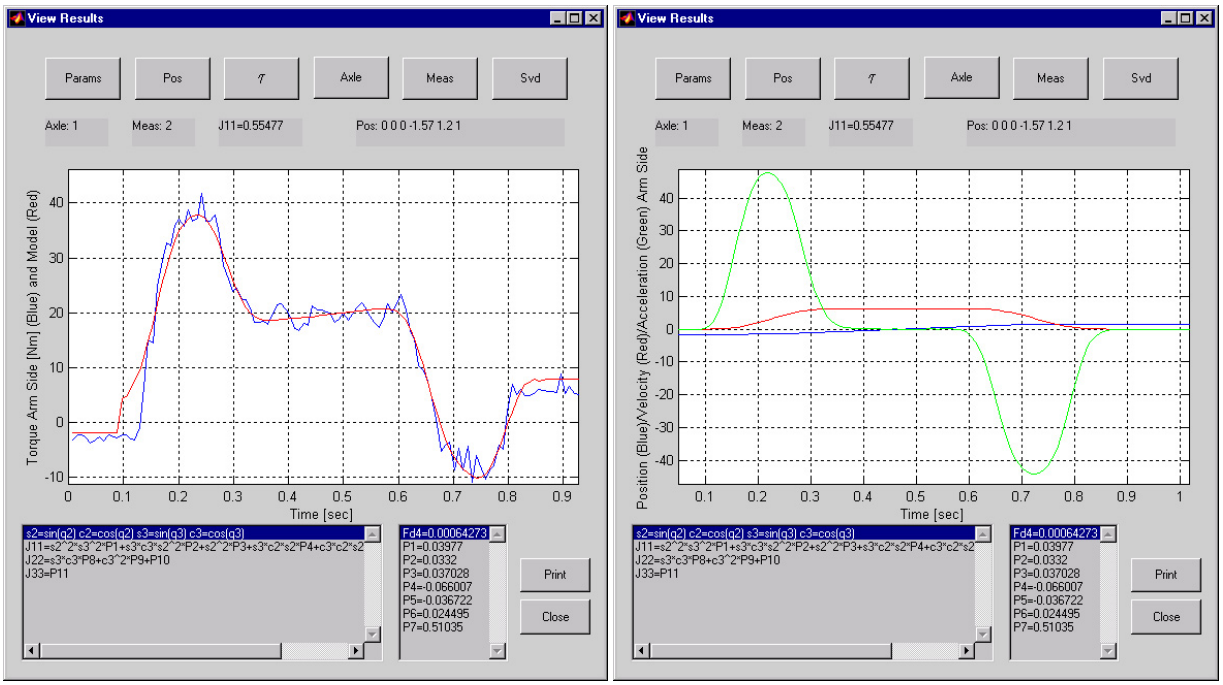

Figure 2: *Measurements from a 3-dof wrist of an ABB industrial robot. The figure on the left shows the measured torque for the first axis in Nm (noisy) and the corresponding modelled torque, given by equation (1). The figure on the right shows the measured position, velocity and acceleration for a ramp response in axis one.*

where C_{jk} is a diagonal 3×3 matrix with the Coloumb friction elements on the diagonal.

The identification of the physical parameters is divided into two steps. First, gravity, Coriolis, centripetal and inertia terms are identified for a given configuration of the wrist. Second, a series of identification results from step one are joined together to solve individual terms of the type PJ_1, PJ_2, etc. Some other solutions, for example [11], combine these two steps into one and perform the entire identification in one step. The advantage of dividing the identification into two steps, is that we can isolate individual physical terms, such as inertia, and check that we have persistent excitation for each of these terms.

The second step of the identification is a linear identification problem, and is well-known in the literature. Here we give a brief example of the identification of J_{11} in section 2.2. If we define the following vectors

$$P = [PJ_1 \ PJ_2 \ PJ_3 \ PJ_4 \ PJ_5 \ PJ_6 \ PJ_7]^T \text{ and } \phi = [s_3^2 s_2^2 \ \ s_3 c_3 s_2^2 \ \ s_2^2 \ \ s_2 c_2 s_3 \ \ c_2 s_2 c_3 \ \ c_2 s_2 \ \ 1] \quad (2)$$

then we can write $J_{11} = \phi P$. Let Φ be a matrix consisting of rows of different ϕ's from different excitation trajectories of the wrist. Then, the identification of P is simply given by $P = \Phi^+ J_{11}$, where $^+$ denotes the pseudo-inverse given by $A^+ = (A^T A)^{-1} A^T$, see [10, 11]. To get correct values for the parameter vector P, it is important to have persistent excitation in the trajectories. In other words, the matrix Φ needs a full rank, in this example a rank of 7. In our experiments, we defined 8 different wrist trajectories for the identification of J_{11} and computed the singular values of the matrix Φ. The singular values were found to be 3.63,1.28,0.86,0.73,0.59,0.31 and 0.30. From experimentation, we found the path trajectories to be acceptable when the smallest singular value of Φ was within approximately 10% of the largest singular value.

Figure 2 shows some of the final identified parameters. For example, the inertia of first axis of the wrist is identified as

$$J_{11} = 0.0398 s_3^2 s_2^2 + 0.0332 s_3 c_3 s_2^2 + 0.0370 s_2^2 - 0.0660 s_2 c_2 s_3 - 0.0367 c_2 s_2 c_3 + 0.0245 c_2 s_2 + 0.5104 \quad (3)$$

which gives 7 of the 25 parameters appearing in the 18 linearly independent equations, ie. $PJ_1 = 0.0398$, $PJ_2 = 0.0332$, $PJ_3 = 0.0370$, $PJ_4 = -0.0660$, $PJ_5 = -0.0367$, $PJ_6 = 0.0245$, $PJ_7 = 0.5104$. In addition

to these 7 parameters, the following parameters can also be identified by running experiments on the wrist: PG_1, PG_2, PG_3, PG_4, PG_5, PG_6, PJ_{10}, PJ_{13}, PJ_{16}, PJ_{19} and PS_3. Together with 7 physical parameters estimated before assembly of the wrist (${}^a m$,${}^b m$, ${}^b l_1$, ${}^b t_2$, ${}^c t_1$, ${}^b J_{33}$ and ${}^c J_{33}$), the remaining 18 physical parameters can all be identified.

6 Conclusions

In this paper we have demonstrated rigid-body dynamics modelling and methods for verification and identification of an industrial ABB robot wrist. The derivation of the equations was done in Maple using Sophia and Kane's method. With these tools, even the equations for complex 6-dof manipulators can be derived quickly.

For verification, linear combinations of the wrist parameters can be identified and compared with CAD data of the wrist. If the identified parameters and the CAD data show large differences, then the CAD data can be modified or individual parts in a disassembled wrist can be measured more precisely using external measuring devices in an attempt to make the correspondance better.

For identification, 32 physical parameters were included in the original model, where 25 of these appear in the dynamic equations of motion. Of these 25 parameters, we are able to identify 18 parameters, given initial estimates of the remaining 7 parameters. The methods presented in the paper have been tested with experiments on an ABB industrial wrist with internal transmission couplings. The identification methods are used at ABB today to improve a) the robots path tracking performance, b) the input data to dynamic simulation tools c) drive system optimization and the mechanical design of the arm structures.

References

[1] Armstrong-Hélouvry, B., *Control of Machines with Friction*, Kluwer Academic Publishers, 1991.

[2] Atkeson C.G., C.H. An and J.M. Hollerbach, "Estimation of Inertial Parameters of Manipulators Loads and Links", *International Journal of Robotics Research*, Vol. 5, No. 3, pp. 101-118, 1986.

[3] Craig, J.J., *Introduction to Robotics: Mechanics and Control*, J. J. Craig, Addison-Wesley, 1989.

[4] Fung, Y.C., *Foundations of Solid Mechanics*, Prentice-Hall, Inc., 1965.

[5] Gautier M., "Dynamic Identification of Robots with Power Model", *Proceedings of the 1997 IEEE International Conference on Robotics and Automation (ICRA '97)*, Albuquerque, 20-25 April 1997, pp. 1922-1927.

[6] Kane T.R. and D.A. Levinson, "*Dynamics: Theory and Applications*", McGraw-Hill 1985.

[7] Lennartsson A. "*Efficient Multibody Dynamics*", Doctorial Thesis, Royal Institute of Technology, Stockholm, Sweden, 1999. TRITA-MEK, Technical Report 1999:01, ISSN 0348-467X.

[8] Lesser M., "*The Analysis of Complex Nonlinear Mechanical System*", World Scientific Series on Nonlinear Science, Series A Vol.17, World Scientific Publishing Co. 1995.

[9] Reyes F. and R. Kelly, "On Parameter Identification of Robot Manipulators", *Proceedings of the 1997 IEEE International Conference on Robotics and Automation (ICRA '97)*, Albuquerque, 20-25 April 1997, pp. 1910-1915.

[10] Strang, G., *Linear Algebra and Its Applications*, Harcourt Brace Jovanovich, 1988.

[11] Swevers J., et.al., "Optimal Robot Excitation and Identification", *IEEE Transactions on Robotics and Automation*, Vol. 13, No. 5, Oct. 1997, pp. 730-740.